INTERNATIONAL ATOMIC ENERGY AGENCY
UNITED NATIONS EDUCATIONAL, SCIENTIFIC AND CULTURAL ORGANIZATION
INTERNATIONAL CENTRE FOR THEORETICAL PHYSICS
I.C.T.P., P.O. BOX 586, 34100 TRIESTE, ITALY, CABLE: CENTRATOM TRIESTE

SMR/697-4

RESEARCH WORKSHOP ON CONDENSED MATTER PHYSICS

(21 June - 3 September 1993)

WORKING PARTY ON SMALL SEMICONDUCTOR STRUCTURES

(2 - 13 August 1993)

OPTICAL SPECTROSCOPY OF TYPE I AND TYPE II SUPERLATTICES

E. L. IVCHENKO
Academy of Sciences
A.F. Ioffe Physical-Technical Institute
Polytechnicheskaya 26
194021 St. Petersburg
Russian Federation

These are preliminary lecture notes, intended only for distribution to participants

OPTICAL SPECTROSCOPY OF TYPE I AND TYPE II SUPERLATTICES

E.L.Ivchenko, A.F.Ioffe Physico-Technical Institute, St.Petersburg, Russia

1. Principles of Optical Orientation
2. Suppression of Free-Carrier Spin Relaxation in Classical Magnetic Fields (in Type I SLs)
3. Optical Orientation of Excitons in Type II GaAs/AlAs SLs in Longitudinal Magnetic Fields
4. Mystery of Anisotropic Exchange Splitting of the Radiative Excitonic Doublet in Type II GaAs/AlAs SLs
5. ΓX Mixing of Electron States in $(GaAs)_N(AlAs)_M$ SLs
6. Spin-Flip Raman Scattering from Holes Bound to Acceptors in $GaAs/Al_xGa_{1-x}As$ MQWs

OPTICAL SPECTROSCOPY OF TYPE I AND TYPE II SLs (references)

E.L.Ivchenko

Reflection

- Exciton Longitudinal-Transverse Splitting in GaAs/AlGaAs SLs and MQWs (with Kochereshko, Kop'ev, Kosobukin, Uraltsev, and Yakovlev, *Solid State Commun.* 70, 529, 1989)
- Exciton Oscillator Strength in Magnetic Field Induced Spin SLs CdTe/(Cd,Mn)Te (with Kavokin, Kochereshko, Pozina, Uraltsev, Yakovlev, Bichnell-Tassius, Waag, and Landwehr, *Phys.Rev. B*46, 7713, 1992)
- Excitonic Polaritons in Periodic QW Structures (*Sov.Phys.Solid State* 33, 1344, 1991)
- Exciton Resonance Reflection from QW, Quantum Wire and Quantum Dot Structures (with Kavokin, Kochereshko, Kop'ev, and Ledentsov, *Superlatt.Microstruct.* 12, 317, 1992)

Absorption

-Absorption Coefficient in Type-II GaAs/AlAs Short-Period SLs (with Voliotis, Grousson, Lavallard, Kiselev, and Planel, to be published)

-Electron Minibands in $(GaAs)_N(AlAs)_M$ SLs for Even and Odd M (with Aleiner, *Sov.Phys.Semicond.*, 1993)

Photoluminescence

- Exciton Parameters and Electron Miniband Structure of GaAs/AlGaAs (with Uraltsev, Kop'ev, Kochereshko, and Yakovlev, *Phys.Stat.Sol.(b)* 150, 673, 1988)
- Magnetic-Field-Effects on Photoluminescence Polarization in Type II GaAs/AlAs SLs (with Kochereshko, Naumov, Uraltsev, and Lavallard, *Superlatt.Microstruct.* 10, 497, 1991)
- Nature of Anizotropic Exchange Splitting in Type II GaAs/AlAs SLs (with Aleiner, *JETP Letters* 55, 692, 1992)
- Electron g-Factor in QWs and SLs (with Kiselev, *Sov.Phys.Semicond.* 26, 827, 1992)
- Tunneling Current Bistability and Photoluminescence in a Triple-Barrier Structure (with Kiselev, Zou, and Willander, *Sov.Phys.Semicond.*, 1993, to be published)

Spin-Flip Raman Scattering

- Spin-Flip Raman Scattering in $GaAs/Al_xGa_{1-x}As$ MQWs (with Sapega, Cardona, Ploog, and Mirlin, *Phys.Rev. B*45, 4320, 1992)
- Exchange Interaction and Light Scattering Due to Spin-Flip of Holes Bound to Acceptors in QW Structures (*Sov.Phys.Solid State* 34, 254, 1992)

Nonlinear Optics and Photogalvanic Effects

- Reflectivity and Photoreflectivity in SLs and QWs (with Kochereshko, Uraltsev, and Yakovlev, *Phys.Stat.Sol. (b)* 161, 217, 1990)
- Current of Thermalized Spin-Oriented Photocarriers (with Lyanda-Geller and Pikus, *Sov.Phys.JETP* 71, 1155, 1990)

PRINCIPLES OF OPTICAL ORIENTATION

1. Under optical interband excitation by circularly polarized light, the angular momenta of σ_+ (or σ_-) photons are transformed to angular momenta (or spin) of free carriers:

$$s_z^{\circ} \propto P^{\circ}_{circ} = \frac{I^{\circ}_{\sigma_+} - I^{\circ}_{\sigma_-}}{I^{\circ}_{\sigma_+} + I_{\sigma_-}}$$

GaAs/AlGaAs
SQW or SL

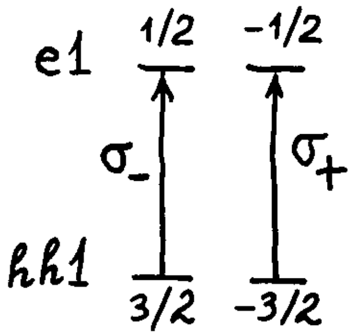

2. If the photoelectron lifetime, τ_0, is not too long as compared to the spin relaxation time, τ_s, then the photoelectrons retain spin polarization (at least partially) under steady-state excitation

$$S_z = \frac{\tau_s}{\tau_s + \tau_0} S_z^{\circ} = \frac{S_z^{\circ}}{1 + \frac{\tau_0}{\tau_s}}$$

3. The radiative recombination of spin-polarized carriers is manifested by emission of circularly polarized photons

$$P_{circ} \propto S_z$$

Principles of Optical Orientation-2

4. The transverse magnetic field leads to depolarization of the photoluminescence

$$\mathcal{H}_{\vec{B}} = \frac{1}{2} g \mu_0 (\vec{\sigma} \cdot \vec{B}) = \frac{1}{2} \hbar (\vec{\sigma} \vec{\Omega}_L)$$

Pauli matrices

Zeeman interaction; electron g-factor; Bohr magneton; Larmor frequency

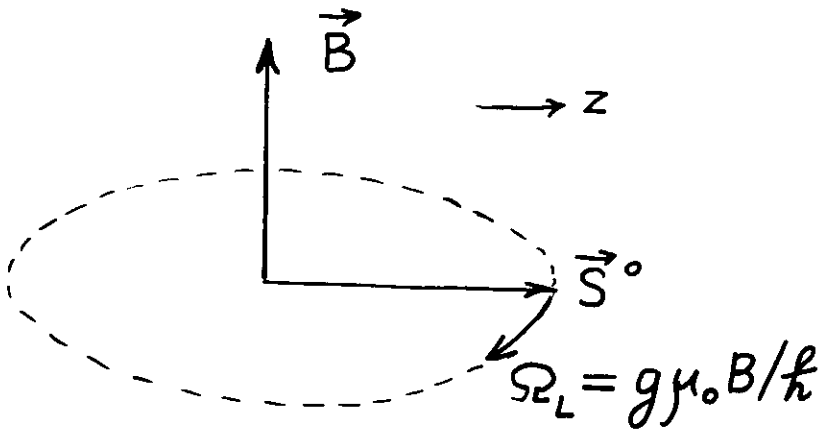

$$S_z(B) = \frac{S_z(0)}{1+(\Omega_L T)^2}$$

$$\frac{1}{T} = \frac{1}{\tau_0} + \frac{1}{\tau_s}$$

5. Excitons can be oriented as well as free carriers, under circularly polarized excitation. Under resonant excitation by linearly polarized light, excitons are generated with an oscillating dipole moment aligned along the polarization plane (optical alignment of excitons)

$$P_{lin} = \frac{I_x - I_y}{I_x + I_y} \propto P^\circ_{lin}$$

SUPPRESSION OF FREE-CARRIER SPIN RELAXATION IN LONGITUDINAL MAGNETIC FIELDS

The Dyakonov-Perel spin relaxation due to $\vec{k}$-dependent splitting of electron spin states

Bulk GaAs

$$\mathcal{H}_{so} = \gamma\left[\sigma_x k_x (k_y^2 - k_z^2) + \sigma_y k_y (k_z^2 - k_x^2) + \sigma_z k_z (k_x^2 - k_y^2)\right]$$

$GaAs/Al_xGa_{1-x}As$ (001)

SQW or SL

$$\mathcal{H}_{so} = \gamma \langle k_z^2 \rangle \left(-\sigma_x k_x + \sigma_y k_y\right),$$

where

$$\langle k_z^2 \rangle = \int \varphi(z)\left(-\frac{\partial^2}{\partial z^2}\right)\varphi(z)\, dz$$

Electron envelope function

In a SQW

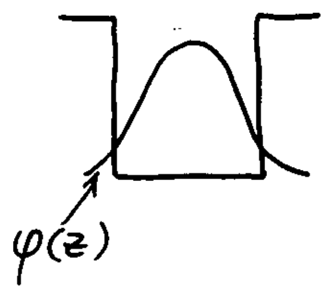

In a SL, $\varphi(z+d) = \varphi(z)$

In (001) heterostructures

$$\Omega_{\vec{k},x} = -\frac{2}{\hbar}\gamma\langle k_z^2\rangle k_x$$

$$\Omega_{\vec{k},y} = \frac{2}{\hbar}\gamma\langle k_z^2\rangle k_y$$

$$\Omega_{\vec{k},z} = 0$$

$$\mathcal{H}_{so} = \frac{\hbar}{2}(\vec{\sigma}\vec{\Omega}_{\vec{k}})$$

Effective Larmor frequency

The value and direction of $\Omega_{\vec{k}}$ depends on $\vec{k}$

FREE-CARRIER SPIN RELAXATION - 2

Random rotations of electron spin vector

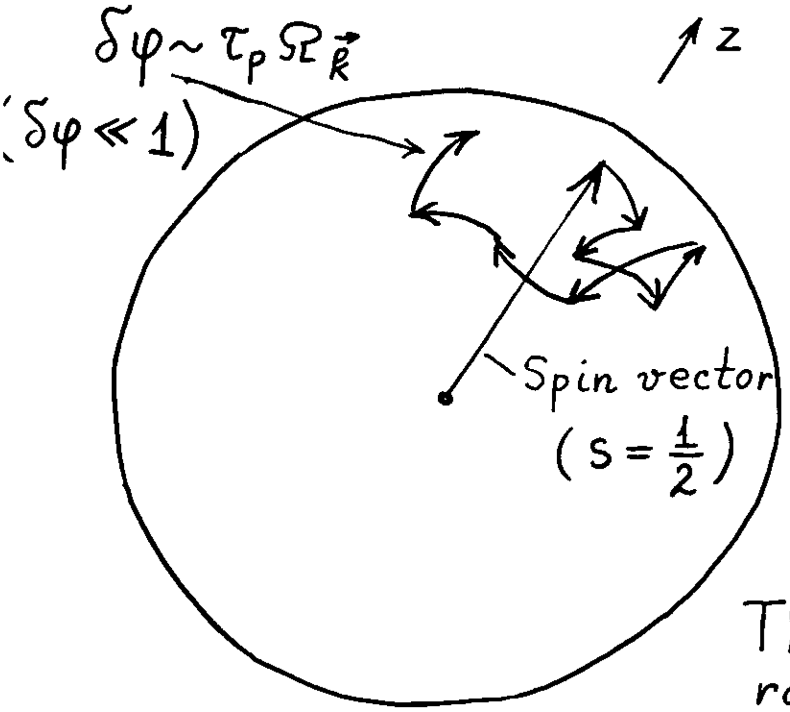

Number of momentum scattering events within the time interval t :

$$n = \frac{t}{\tau_p}$$

The average squared rotation angle

$$\overline{(\Delta\varphi)^2} \sim \sum_i \overline{(\delta\varphi_i)^2} \sim \frac{t}{\tau_p}(\delta\varphi)^2 \sim t\,\tau_p \overline{(\Omega_{\vec{k}}^2)}$$

By definition, $\tau_s \tau_p \overline{(\Omega_{\vec{k}}^2)} \sim 1$ or $\frac{1}{\tau_s} \sim \tau_p \overline{(\Omega_{\vec{k}}^2)}$

For QWs or SLs,

$$\frac{1}{\tau_s} = \left(\frac{2}{\hbar}\gamma \langle k_z^2 \rangle\right)^2 k_\perp^2 \tau_p \qquad (k_\perp^2 = k_x^2 + k_y^2)$$

Due to the cyclotron rotation $\left(\omega_c = \frac{eB}{m^* c}\right)$ in the longitudinal magnetic field $\vec{B} \parallel z$ the electron wave vector $\vec{k}$ is time-dependent

$$k_x = k_\perp \cos(\omega_c t + \varphi_0)$$
$$k_y = k_\perp \sin(\omega_c t + \varphi_0)$$

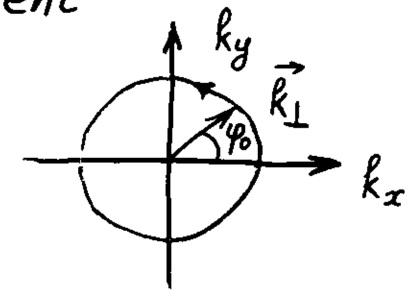

Thus, in the longitudinal magnetic field vector $\Omega_{\vec{k}}$ also varies in time. The values of $\Omega_{\vec{k}(t),x}$ and $\Omega_{\vec{k}(t),y}$ averaged over the cyclotron orbit are zeros. If $\omega_c \tau_p \gg 1$ (strong classical magnetic fields), then the vector $\Omega_{\vec{k}(t)}$ is oscillating in time so rapidly that the electron spin cannot follow this variation and stops to rotate

$$\frac{1}{\tau_s(B_{\parallel})} = \frac{1}{\tau_s(0)} \frac{1}{1+(\omega_c \tau_p)^2}$$

This allows to measure the transport time τ_p by using purely optical methods (The best fit in Fig. 5 below is obtained for $\tau_p = 9ps$)

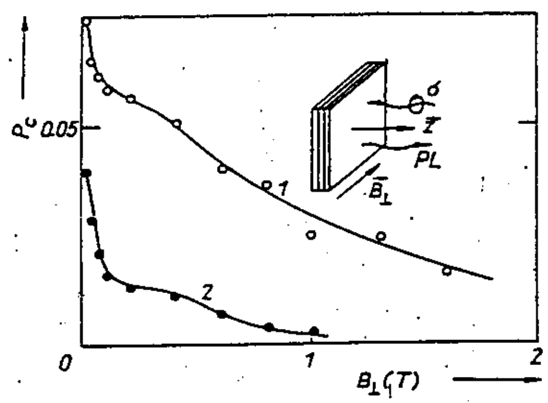

Fig. 4. Hanle depolarization shapes are taken at the PL energies shown by marks in Fig. 3 in the presence of magnetic field in Voigt configuration as the insert shows. Solid lines are calculated according to (3) with $\rho_1 = 0.016$ and 0.025, $\varrho_2 = 0.06$ and 0.015, $B^1_{1/2} = 0.027$ and 0.028T, $B^2_{1/2} = 0.95$ and 0.65T, for the short- and long-wavelength tail of the PL line, respectively

Uraltsev, Ivchenko et al. 1988

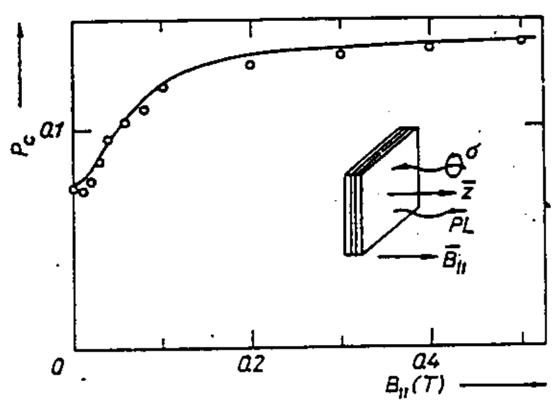

Fig. 5. The increase of contribution to P_c from optical orientation, which is $P_c^\sigma = [P_c(\sigma^+, B_\parallel) - P_c(\sigma^-, B_\parallel)]/2$, is measured in the presence of magnetic field in Faraday configuration at the short-wavelength tail of the PL line. Solid line calculated according to (4)

QUANTUM CONFINEMENT OF FREE CARRIERS IN QWs

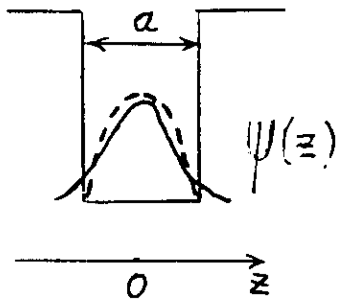

Infinite Barriers

e1: $\psi(z)=\sqrt{\frac{2}{a}}\cos\frac{\pi z}{a}$; $E_{e1}=\frac{\hbar^2}{2m^*}\left(\frac{\pi}{a}\right)^2$

Finite Barriers

$$\psi(z)=\begin{cases} C\cos kz & \text{inside} \\ \mathcal{D}\,e^{-\varkappa\left(|z|-\frac{a}{2}\right)} & \text{outside}\end{cases}$$

QUASI-2D EXCITON

Type I

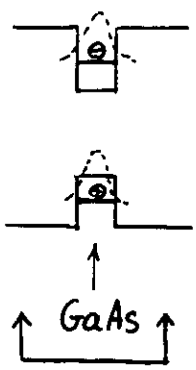

$Al_{0.35}Ga_{0.65}As$

$(CdTe/Cd_{1-x}Mn_xTe)$

Type II

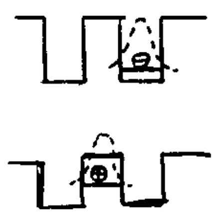

Exciton Envelope Function

$$\Psi_{exc}=F(\rho)\,\psi_{e1}(z_e)\,\psi_{h1}(z_h)$$

GaAs/AlAs SL

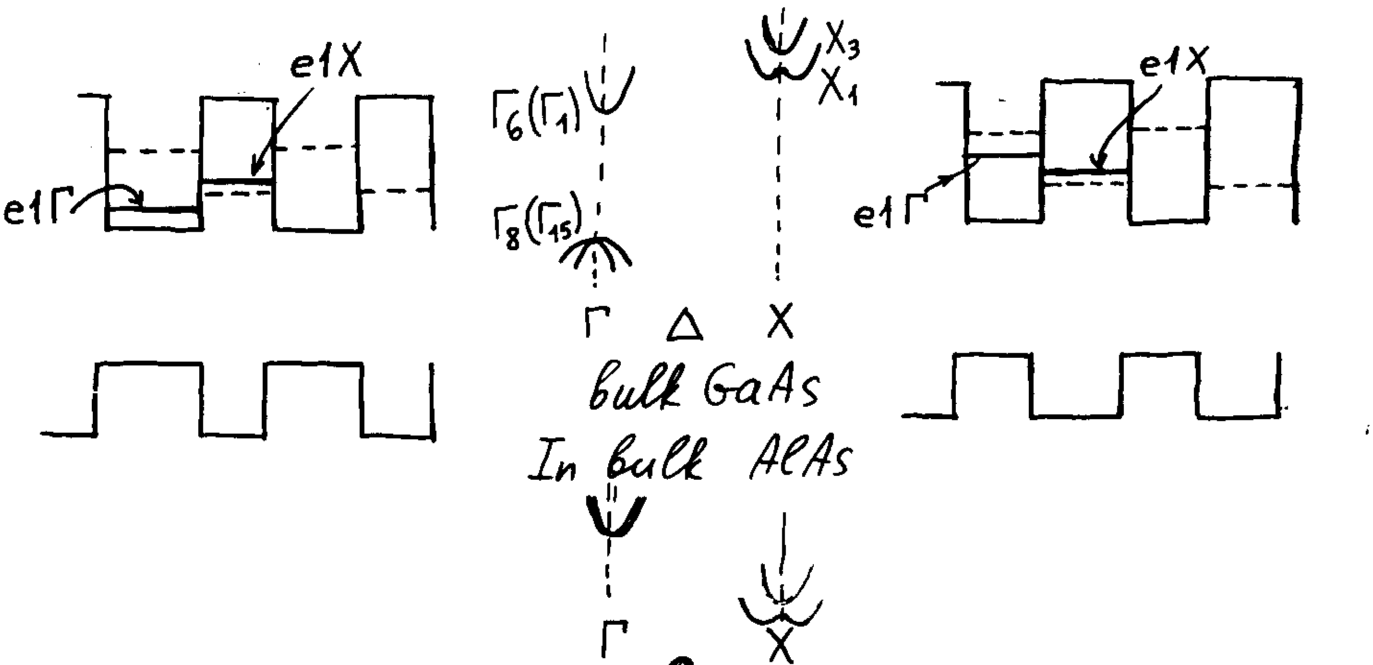

NATURE OF THE LOWEST ELECTRON STATE IN GaAs/AlAs SLs

[1] Danan et al. 1987

[2] van Kesteren et al. 1989

[3] Scalbert et al., Solid State Commun. 70, 945, 1989

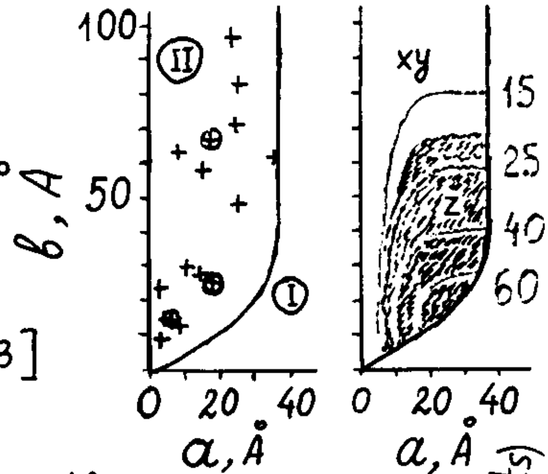

[3]

PL Excitation Spectrum

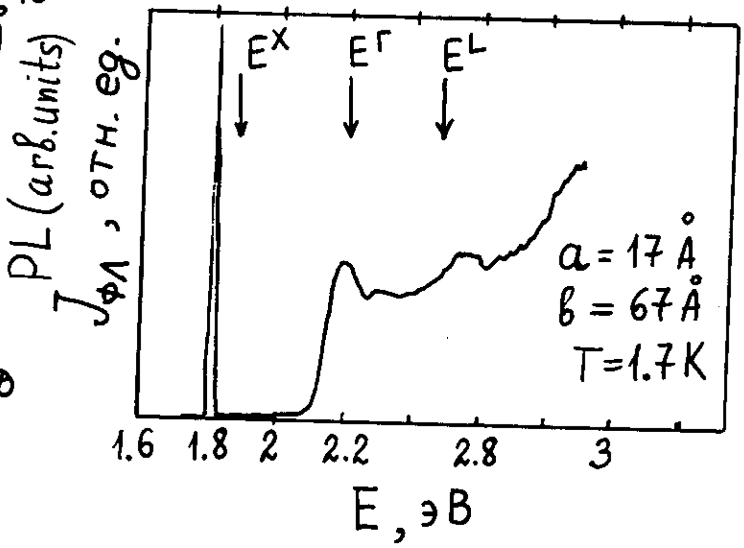

[1]

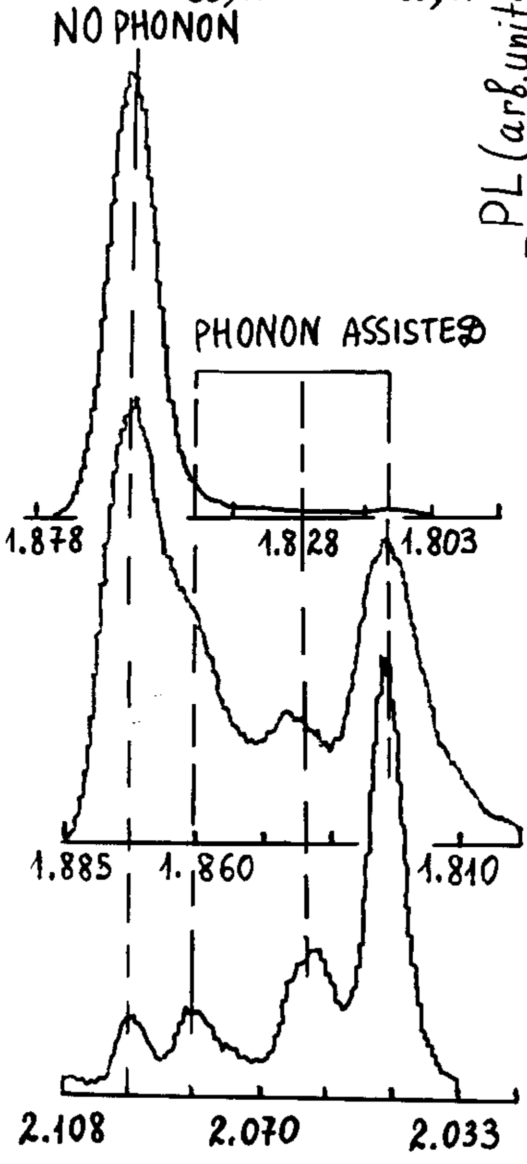

[3]

PL spectra (eV)

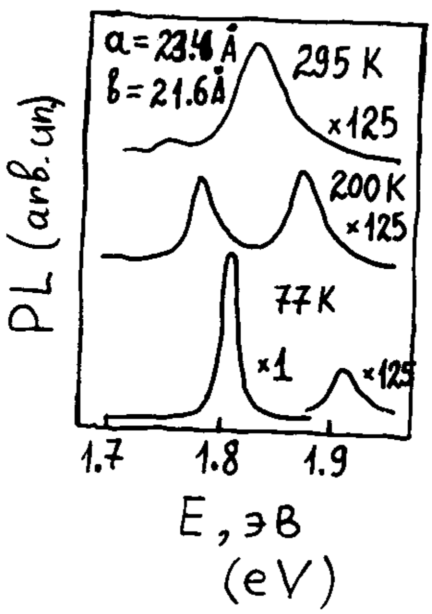

[1]

OPTICAL ORIENTATION OF EXCITONS IN TYPE II GaAs/AlAs SLs IN LONGITUDINAL MAGNETIC FIELDS

Depending on the thicknesses a and b of the GaAs and AlAs layers, GaAs/AlAs SLs can be type I and type II

The fine structure of the e1-hh1(1s) exciton in type II SLs

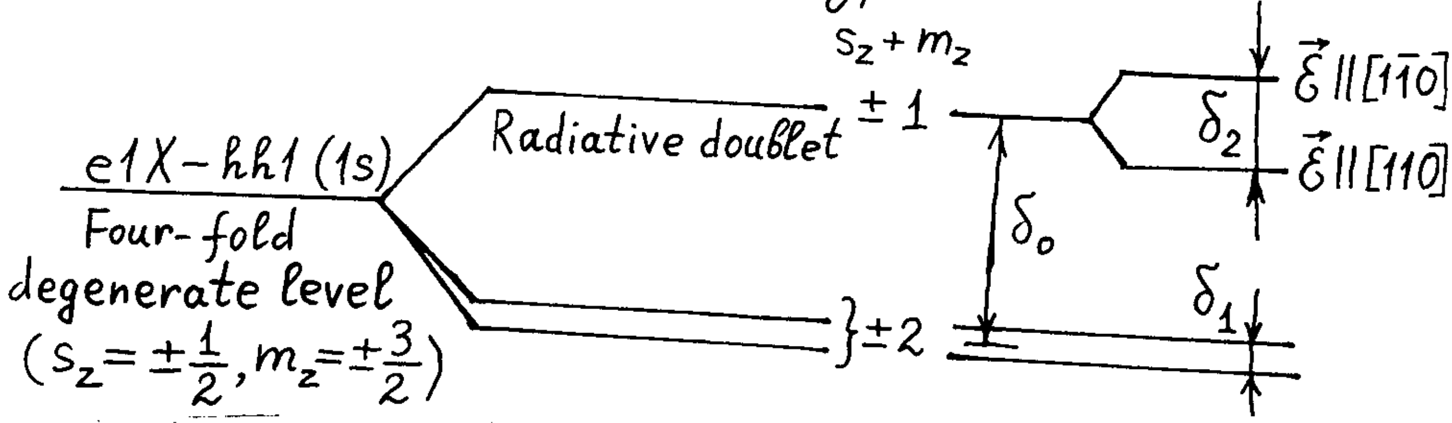

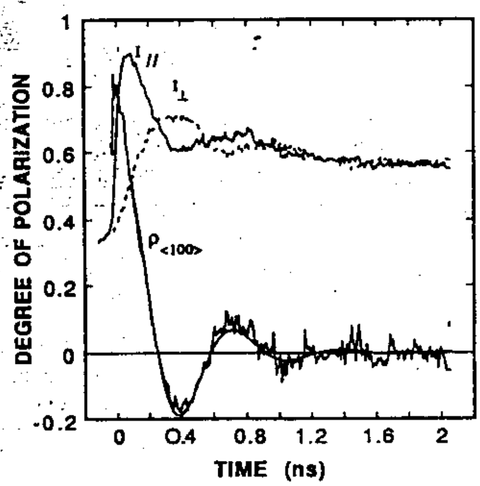

FIG. 1. Degree of polarization $\rho_{\langle 100 \rangle}$ for the composition-graded sample No. 4 in a type-II region close to the type-I–type-II transition [$x=15.7$ mm, composition $\approx(22$ Å)/(11.5 Å)]. The exciting beam is linearly polarized along a $\langle 100 \rangle$ axis. PL intensities $I_{\parallel}$ and $I_{\perp}$ are detected with polarization parallel and perpendicular to the excitation, respectively. $\rho_{\langle 100 \rangle}$ is fitted with $[\rho(0)\exp(-\delta t)\cos(\omega t)]$, where $\hbar\omega=6.3$ μeV, $\hbar\delta=2$ μeV, and $\rho(0)=0.5$. The time origin is taken at the maximum of the $I_{\parallel}$ signal.

Gourdon and Lavallard, 1992

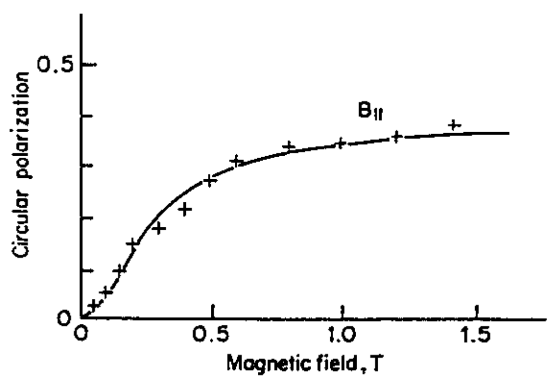

Fig.3 Restoration of circular polarization of the e1-hh1 exciton luminescence in the presence of the longitudinal magnetic field. Solid curve is calculated by using the function $P_{circ}(\infty)[1-L(B)]$, $L(B)$ being the Lorentz-type function with $B_{1/2}=0.25$ T.

Ivchenko et al., SLs & MSs 1991

OPTICAL ORIENTATION OF EXCITONS-2

Linearly Polarized Excitation

Time resolved photoluminescence

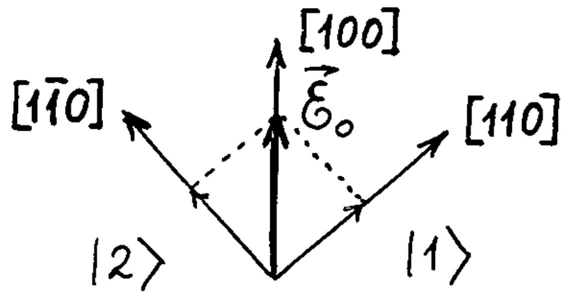

$$|exc,t\rangle \Rightarrow |1\rangle + e^{i\bar{\omega}t}|2\rangle,$$
where $\bar{\omega} = \delta_2/\hbar$

Polarization

$t = 0$: lin $\vec{\mathcal{E}} \parallel [100]$

$\bar{\omega}t = \frac{\pi}{2}$: circ σ_+, $P_{lin} = 0$

$\bar{\omega}t = \pi$: lin $\vec{\mathcal{E}} \parallel [010] \perp \vec{\mathcal{E}}_0$

$\bar{\omega}t = \frac{3}{2}\pi$: circ σ_-

Circularly Polarized Excitation

Steady-state regime

$$|exc,t\rangle \Rightarrow |1\rangle + i\, e^{i\bar{\omega}t}|2\rangle$$

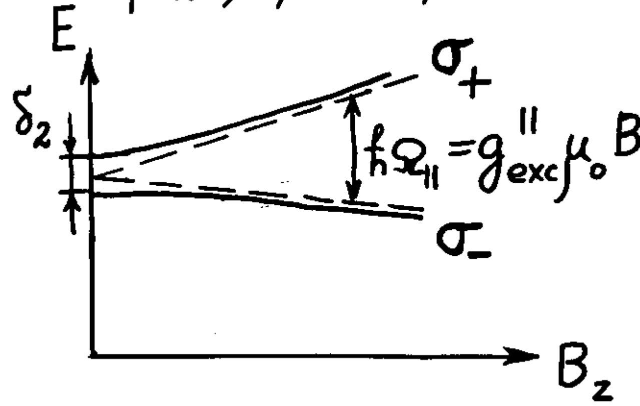

If $\bar{\omega}\tau_0 \gg 1$,
the steady-state circular polarization of the photoluminescence is close to zero

$$P_{circ} = P^0_{circ} \frac{\int_0^\infty dt\, e^{-t/\tau_0} \cos\bar{\omega}t}{\int_0^\infty dt\, e^{-t/\tau_0}} = \frac{P^0_{circ}}{1 + (\bar{\omega}\tau_0)^2} \approx 0$$

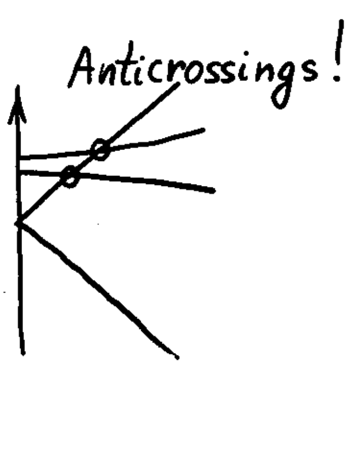

$$P_{circ}(B_{\parallel}) = P^0_{circ} \frac{1 + (\Omega_{\parallel}\tau_0)^2}{1 + (\Omega_{\parallel}^2 + \bar{\omega}^2)\tau_0^2} \approx$$

$$\approx P^0_{circ} \frac{\Omega_{\parallel}^2}{\Omega_{\parallel}^2 + \bar{\omega}^2}$$

Mystery of Anisotropic Exchange Splitting in Type II GaAs/AlAs SLs

In experiment:

(a) Radiative Doublet is split

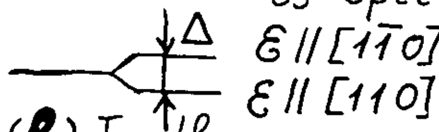

(b) In the same sample there are excitons with $\Delta > 0$ and $\Delta < 0$ (values of $|\Delta|$ coincide)

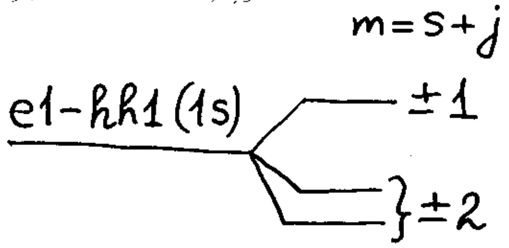

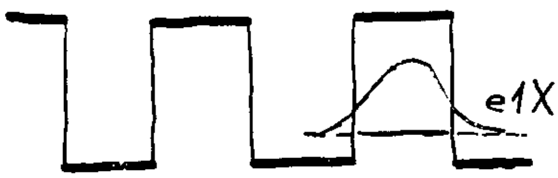

The wave function of a localized exciton

$$\Psi_{exc} = f(\vec{R}_\perp) F(\rho)\, \psi_{e1X}(\vec{r}_e)\, \psi_{hh1}(\vec{r}_h)$$

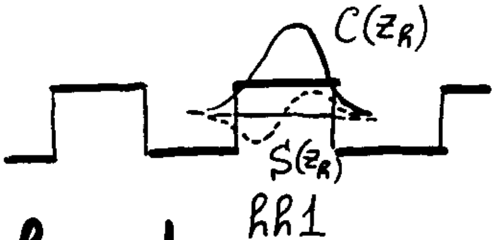

Explanation:

h-l mixing at heteroboundary

$$a_0 \frac{m_0}{m^A_{hh}} \frac{\partial}{\partial z} \varphi^A_{hh,\pm\frac{3}{2}} = a_0 \frac{m_0}{m^B_{hh}} \frac{\partial}{\partial z} \varphi^B_{hh,\pm\frac{3}{2}} + i t_{l-h}\, \varphi^B_{lh,\mp\frac{1}{2}}$$

$$a_0 \frac{m_0}{m^A_{lh}} \frac{\partial}{\partial z} \varphi^A_{lh,\mp\frac{1}{2}} = a_0 \frac{m_0}{m^B_{lh}} \frac{\partial}{\partial z} \varphi^B_{lh,\mp\frac{1}{2}} - i t_{l-h}\, \varphi^B_{hh,\pm\frac{3}{2}}$$

$$\psi_{hh1,\pm 3/2}(\vec{z}_h) = C(z_h)\,|\pm 3/2\rangle \mp i S(z_h)\,|\mp 1/2\rangle$$

$$\underset{\text{exch}}{\text{обм}} = \delta\, \vec{\sigma} \vec{J}\, \delta(\vec{r}_e - \vec{r}_h)$$

$$\frac{\delta_2}{\delta_0} = \frac{\Delta}{\Delta_0} = \frac{4}{\sqrt{3}} \frac{\int dz\, S(z) C(z) \left[u^2(z) + v^2(z)\right]}{\int dz\, C^2(z) \left[u^2(z) + v^2(z)\right]}$$

ANISOTROPIC EXCHANGE SPLITTING

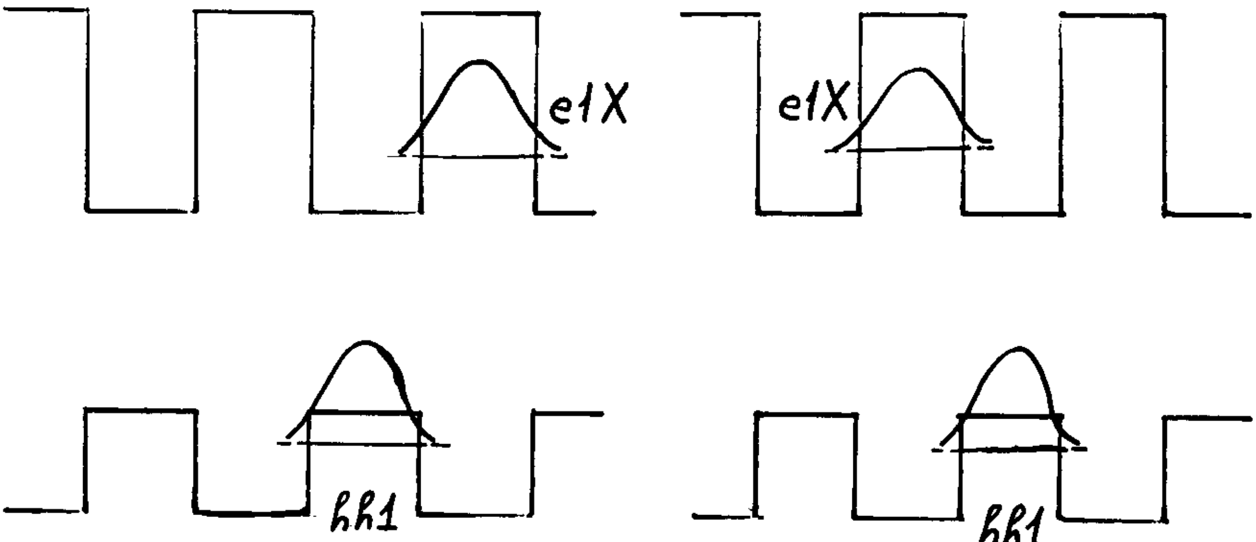

The right-electron exciton

The left-electron exciton

Localized excitons are either right- or left-electron excitons

$$\mathcal{H}_{exch} = \delta(\sigma_x J_x + \sigma_y J_y + \sigma_z J_z)\,\delta(\vec{r}_e - \vec{r}_h)$$

$$\langle -\tfrac{1}{2}, \tfrac{3}{2} | \mathcal{H}_{exch} | \tfrac{1}{2}, -\tfrac{3}{2} \rangle \propto$$

$$\propto \langle -\tfrac{1}{2} | \sigma_x | \tfrac{1}{2} \rangle \langle \tfrac{3}{2} | J_x | -\tfrac{3}{2} \rangle + \langle -\tfrac{1}{2} | \sigma_y | \tfrac{1}{2} \rangle \langle \tfrac{3}{2} | J_y | -\tfrac{3}{2} \rangle$$

$\langle \tfrac{3}{2} | J_{x,y} | -\tfrac{3}{2} \rangle = 0$, if there is no admixture of $\pm 1/2$ to $\pm 3/2$ states!

If the heavy-hole fundamental states hh1, $\pm 3/2$ have an admixture of light-hole states $\pm 1/2$, then the splitting of the radiative exciton doublet is non-zero

$$J_x = \begin{array}{c|cccc} & 3/2 & 1/2 & -1/2 & -3/2 \\ \hline 3/2 & 0 & \sqrt{3}/2 & 0 & 0 \\ 1/2 & \sqrt{3}/2 & 0 & 1 & 0 \\ -1/2 & 0 & 1 & 0 & \sqrt{3}/2 \\ -3/2 & 0 & 0 & \sqrt{3}/2 & 0 \end{array}$$

ANISOTROPIC EXCHANGE SPLITTING-2

$\boxed{1}$ $\pm 3/2$ and $\pm 1/2$ states can be mixed due to a perturbation that has the symmetry of an ε_{xy} shear strain either of an electric field $\mathcal{E}_z$ (Gourdon & Lavallard)

$\boxed{2}$ $\pm 3/2$ and $\pm 1/2$ states are mixed due to the low symmetry, C_{2v}, of a single GaAs/AlAs interface

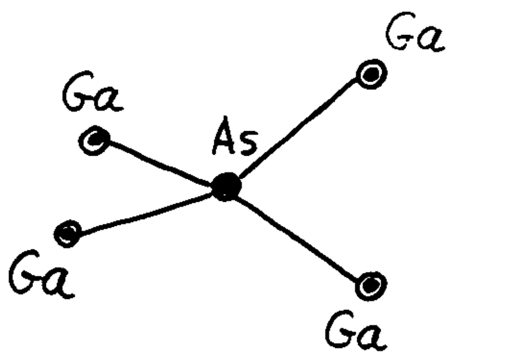

The nearest neighbors of an As atom in GaAs

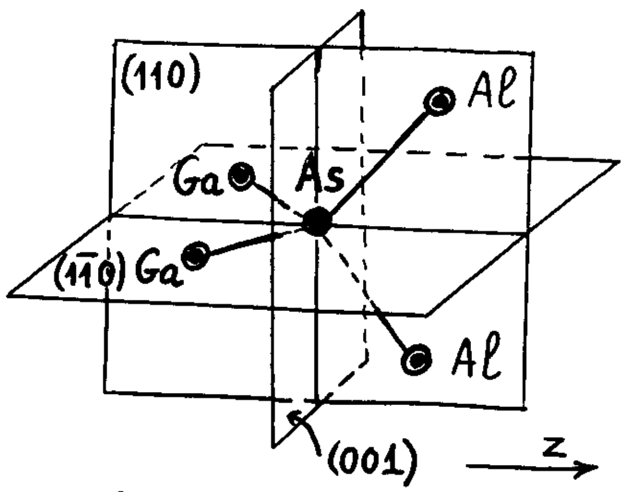

The nearest neighbors of an interface As atom in GaAs/AlAs heterostructures

The symmetry of an ideal heterostructure allows mixing of heavy-hole and light-hole states even when a hole is incident normally on an interface

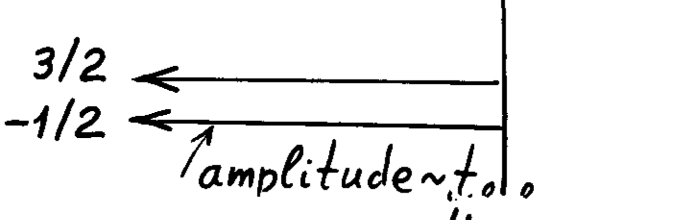

ANISOTROPIC EXCHANGE SPLITTING-3

$$\psi_{hh1,\pm 3/2}(\vec{r}_h) = C(z_h)\,|\pm 3/2\rangle \mp i\,S(z_h)\,|\mp 1/2\rangle$$

In a GaAs layer

$$C(z) = F_h \cos(k_h z) \qquad S(z) = F_\ell \sin(k_\ell z)$$

In the neighboring AlAs layers

$$C(z) = F_h \cos(k_h a/2)\, \exp[-\varkappa_h(|z| - a/2)]$$

$$S(z) = \pm F_\ell \sin(k_\ell a/2)\, \exp[-\varkappa_\ell(|z| - a/2)]$$

$$k_h = (2 m_{hh} E_{hh1}/\hbar^2)^{1/2} \qquad k_\ell = (2 m_{\ell h} E_{\ell h1}/\hbar^2)^{1/2}$$

$$\varkappa_h = [2 m_{hh}(V_0^h - E_{hh1})/\hbar^2]^{1/2}$$

$$\varkappa_\ell = (m_{\ell h}/m_{hh})^{1/2}\, \varkappa_h$$

$$\frac{F_\ell}{F_h} = t_{h\text{-}\ell}\, \frac{m_{\ell h}}{m_0}\, \frac{\cos(k_h a/2)}{k_\ell \cos(k_\ell a/2) + \varkappa_\ell \sin(k_\ell a/2)}$$

$$\langle \tfrac{3}{2}|J_x|-\tfrac{3}{2}\rangle \Rightarrow C(z_h)\, S(z_h)\, \sqrt{3}$$

$$\langle -\tfrac{1}{2}|\sigma_x|\tfrac{1}{2}\rangle \Rightarrow \phi_e^2(z_e)$$

$$\frac{\delta_2}{\delta_0} = \frac{4}{\sqrt{3}}\, \frac{\int dz\, S(z) C(z)\, \phi_e^2(z)}{\int dz\, C^2(z)\, \phi_e^2(z)}$$

$$\langle -\tfrac{1}{2}|\sigma_z|-\tfrac{1}{2}\rangle \langle \tfrac{3}{2}|J_z|\tfrac{3}{2}\rangle$$

$$\phi_e^2(z_e)\; C^2(z_h)\; \frac{3}{2}$$

For the left- and right-electron excitons $|\Delta|$ is the same, but Δ differ in sign (the two classes of excitons with $\Delta > 0$ and $\Delta < 0$!)

Ivchenko, Kaminskii, and Aleiner 1993

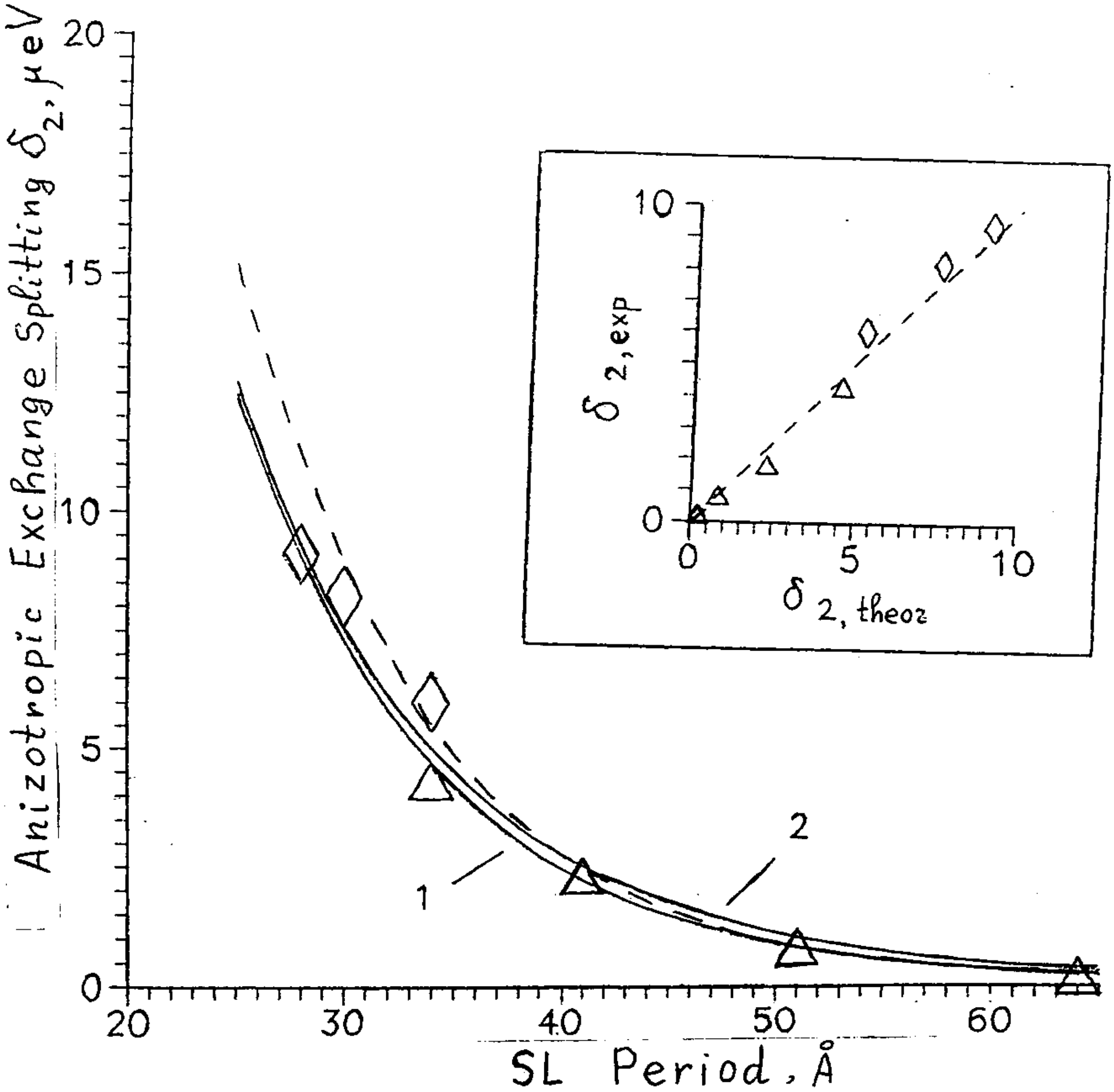

Ivchenko, Kaminskii, and Aleiner 1993

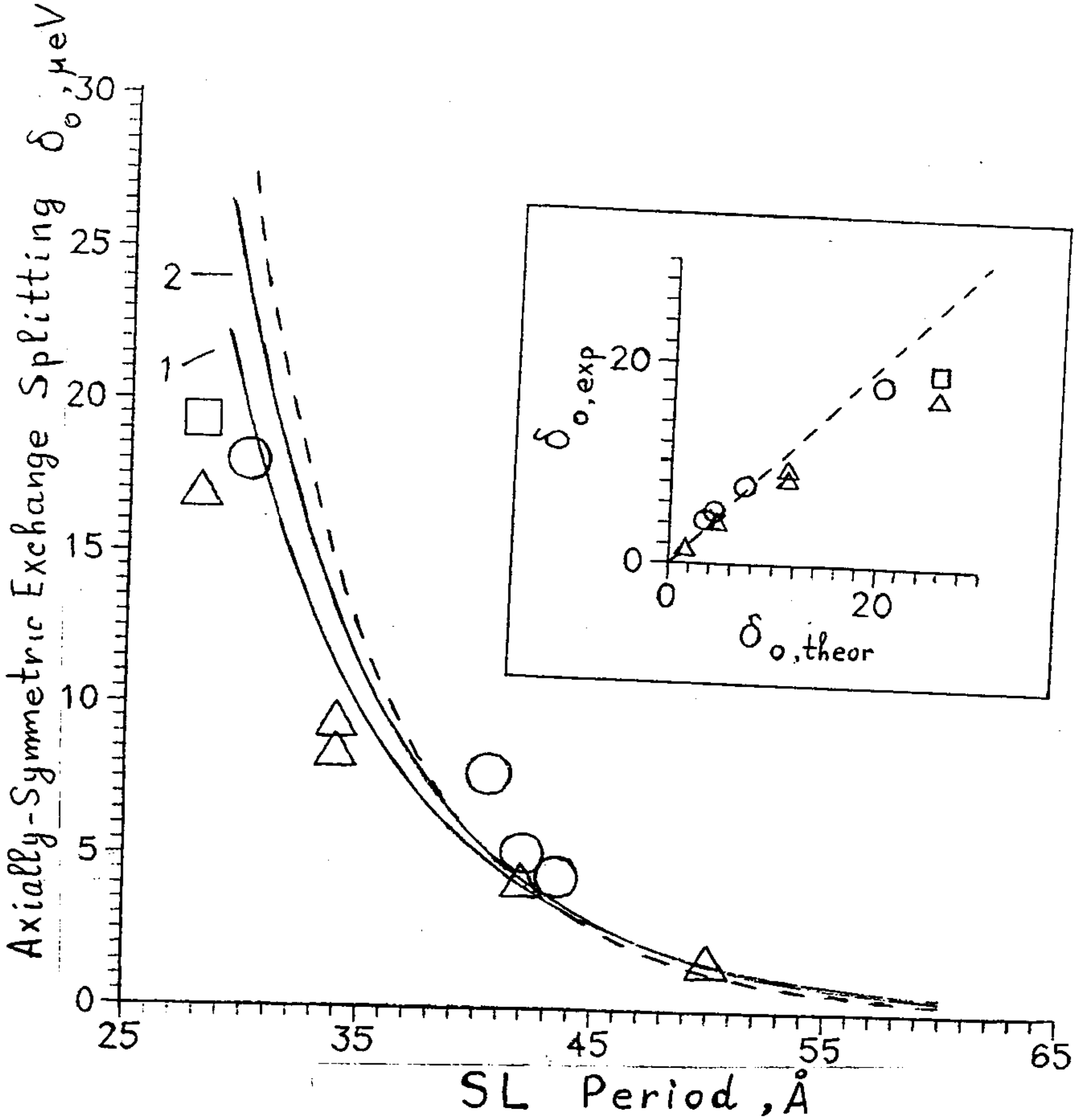

ΓX Mixing of Electron States in $(GaAs)_N(AlAs)_M$ SLs

$$\psi = \underbrace{w(z)\,|\Gamma_1\rangle}_{\psi_\Gamma} + \underbrace{v(z)\,|X_3\rangle + u(z)\,|X_1\rangle}_{\psi_X}$$

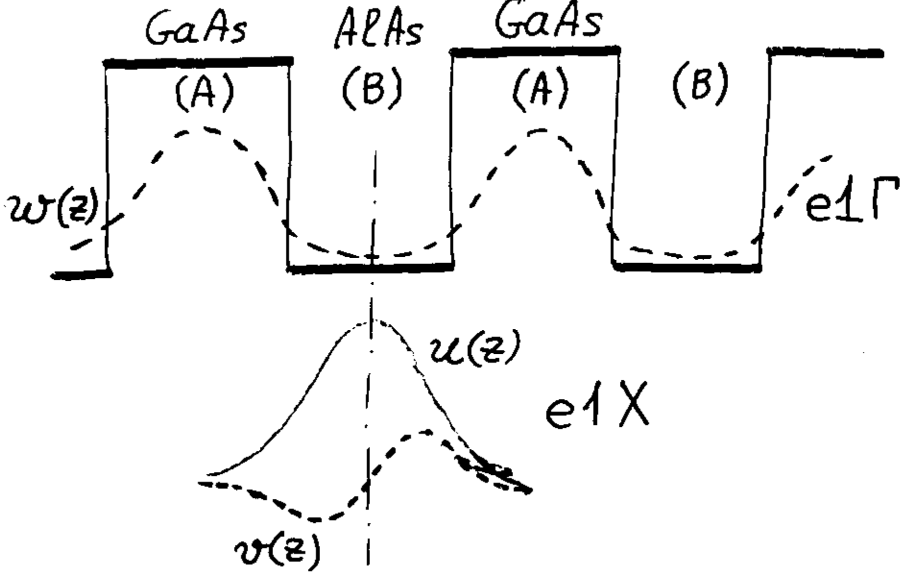

$$a_0 \frac{m_0}{m_\Gamma^A}\frac{\partial}{\partial z} w_A = a_0 \frac{m_0}{m_\Gamma^B}\frac{\partial}{\partial z} w_B + t_{\Gamma X}\,\eta(z_i)\,v_B$$

$$a_0 \frac{m_0}{m_X^{\parallel}}\frac{\partial}{\partial z} v_A = a_0 \frac{m_0}{m_X^{\parallel}}\frac{\partial}{\partial z} v_B + t_{\Gamma X}\,\eta(z_i)\,w_B$$

$\vec{k}_X = \left(0, 0, \frac{2\pi}{a_0}\right)$ $\qquad \eta(z_i) = \cos 2\pi \frac{z_i}{a_0}$

$\vec{a}_3 = \left(\frac{a_0}{2}, 0, \frac{a_0}{2}\right)$ $\qquad V_{\Gamma X} = \sum_i (\pm)\, U a_0\, \eta(z_i)\, \delta(z - z_i)$ $\quad$ + for BA, − for AB

Odd number M $\qquad\qquad$ Even M

GaAsAlAsGa ⟵ Centers of S_{4z} symmetry ⟶ GaAsAlAsAlAsGa

(e1Γ and e1X do not mix at $k_z = 0$) $\qquad$ (e1Γ and e1X do mix at $k_z = 0$)

$$S_{4z}(Al) = t_{\vec{a}_3}\, S_{4z}(As)$$

If $\quad S_{4z}(As)|X_1\rangle = |X_1\rangle$, then $S_{4z}(Al)|X_1\rangle = -|X_1\rangle$

Γ X mixing

ELECTRON TRANSMISSION SPECTRA THROUGH A SINGLE-BARRIER STRUCTURE

GaAs $(AlAs)_M$ GaAs

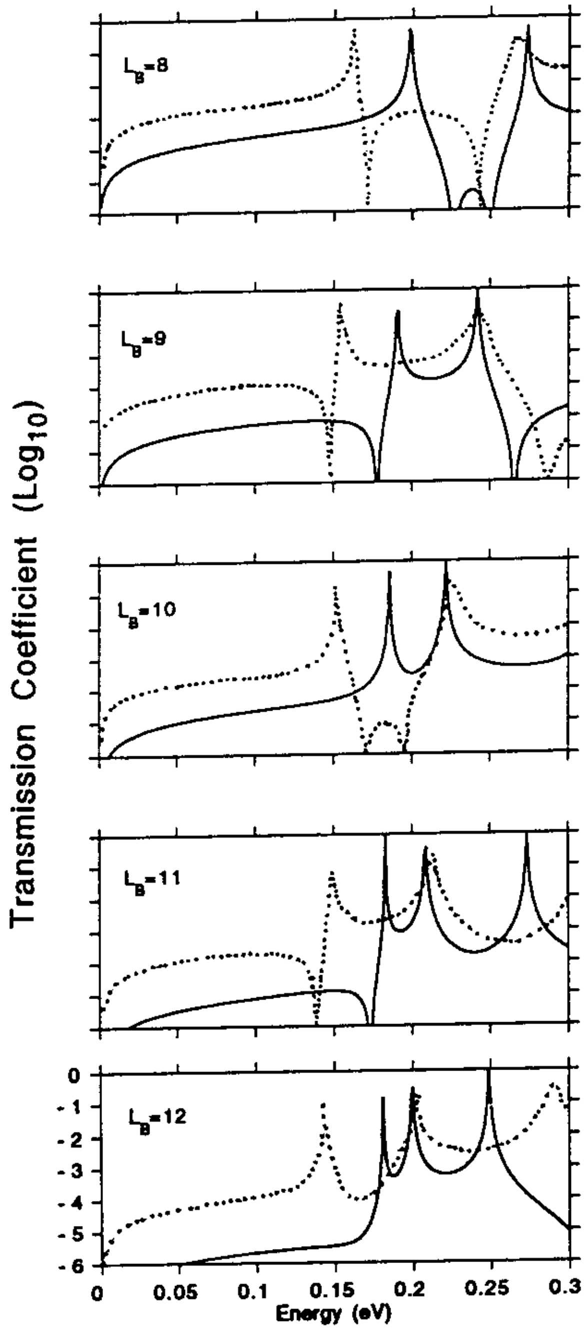

$L_B \equiv M$

Solid curves: Fu, Willander, Ivchenko, and Kiselev (May 1993)

Dotted curves: Ting and McGill (March 1993)

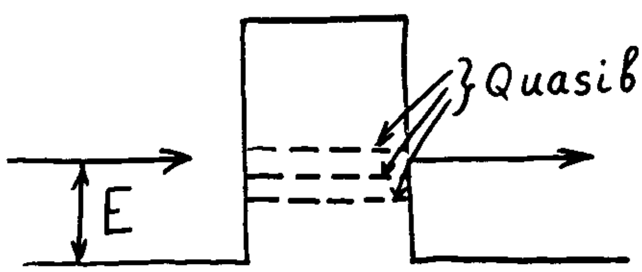

} Quasibound eνX states (ν=1,2...)

ΓX mixing - 2

Electron Miniband Dispersion in $(GaAs)_N(AlAs)_M$ SLs near the Transition from Type I to Type II

$$E_{\pm}(\vec{k}) = \frac{1}{2}\left\{ E_{e1\Gamma}(\vec{k}) + E_{e1X}(k_\perp) \pm \sqrt{\left[E_{e1\Gamma}(\vec{k}) - E_{e1X}(k_\perp)\right]^2 + \bar{V}^2\chi} \right\}$$

$$\chi = \cos^2\left(\frac{k_z d}{2} + \frac{M}{2}\pi\right)$$

$$\bar{V} = \frac{2\hbar^2}{a_0 m_0} w^\circ(BA)\, v^\circ(BA)$$

The parity of AlAs monolayer number, M, is explicitly present in the expression for χ and, hence, in the dispersion $E_\pm(\vec{k})$. When M is even the phase $M\pi/2$ is an integer number of π, $\chi = \cos^2(k_z d/2)$, the states $e1\Gamma$, $e1X$ are mixed at $k_z = 0$ and do not mix at $k_z = \pi/d$. In the case of odd M, $\chi = \sin^2(k_z d/2)$, the ΓX mixing is allowed at the SL Brillouin zone boundary while at $k_z = 0$ the mixing is absent.

ΓX mixing - 3

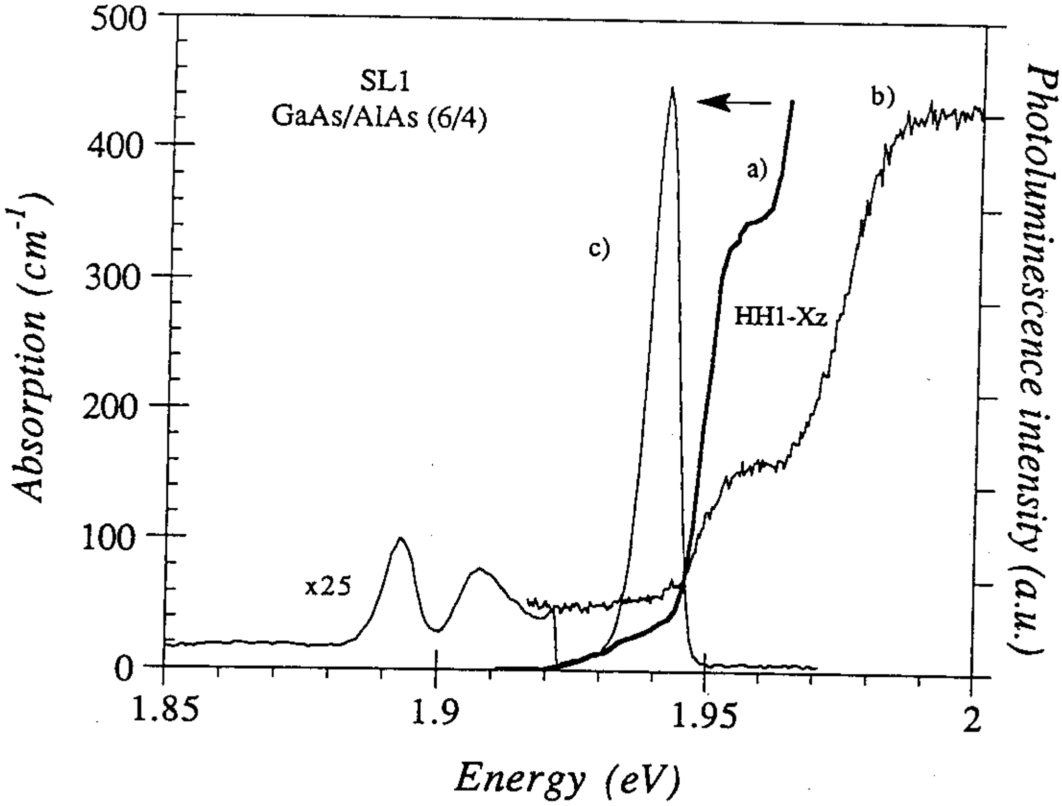

Fig.2. Absorption in the parallel polarization, PLE and PL spectra of SL1 at low temperature. a) the bold solid line represents the absolute absorption curve. The excitonic transition, labelled HH1-X_z lies at 1.954 eV. b) PLE spectrum. c) PL spectrum. The zero-phonon line is shifted by 11 meV from the absorption excitonic peak and two phonon replicas appear at 1.908 and 1.894 eV. The detection energy was set at 1.894 eV and the scanned energy range was between 1.989 and 2.17 eV.

Voliotis, Grousson, Lavallard, Ivchenko, Kiselev, and Planel 1993

Spin-flip Raman scattering in $GaAs/Al_xGa_{1-x}As$ multiple quantum wells

V. F. Sapega,* M. Cardona, and K. Ploog
Max-Planck-Institut für Festkörperforschung, Heisenbergstrasse 1, D-7000 Stuttgart 80, Federal Republic of Germany

E. L. Ivchenko and D. N. Mirlin
A. F. Ioffe Physico-Technical Institute, Academy of Sciences of the U.S.S.R., 194021 Leningrad, U.S.S.R.

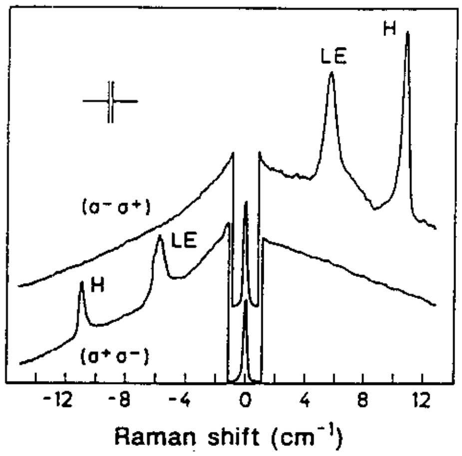

FIG. 2. Raman spectra measured in (σ^-,σ^+) (upper spectrum) and (σ^+,σ^-) (lower) configurations in a magnetic field $B=10$ T and for excitation energies $\hbar\omega=1.628$ eV. H labels the hole spin-flip Raman line, LE the localized exciton angular momentum flip line. Sample 46/110.

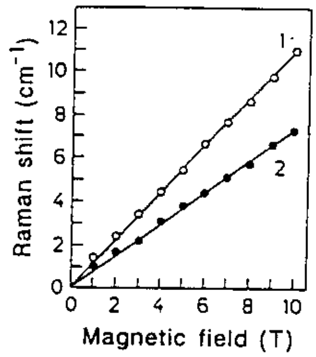

FIG. 3. Dependence of Raman shift on magnetic field strength: (1), SFRS from Be-doped MQW 46/110 (spin flip of hole bound on acceptor). (2), SFRS from undoped MQW 29/101 (angular momenta flip of localized exciton).

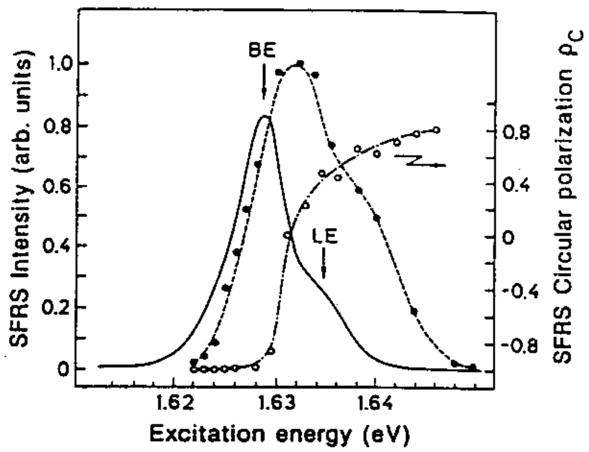

FIG. 1. Resonance profile of the SFRS efficiency for the $z(\sigma^-,\sigma^+ + \sigma^-)\bar{z}$ configuration in a magnetic field $B=10$ T (dashed line, full dots). Photoluminescence spectrum of the MQW 46/110 also for $B=10$ T and excitation at $\hbar\omega=1.7$ eV (solid line). The circles and dashed-dotted line show the dependence of the circular polarization ρ_c on excitation energy ($\rho_c=[I(\sigma^-,\sigma^-)-I(\sigma^-,\sigma^+)]/[I(\sigma^-,\sigma^-)+I(\sigma^-,\sigma^+)]$, where $I(\sigma^-,\sigma^-)$ and $I(\sigma^-,\sigma^+)$ are the intensities of the Raman lines measured in (σ^-,σ^-) and (σ^-,σ^+) configurations).

SPIN-FLIP RAMAN SCATTERING FROM HOLES BOUND TO ACCEPTORS

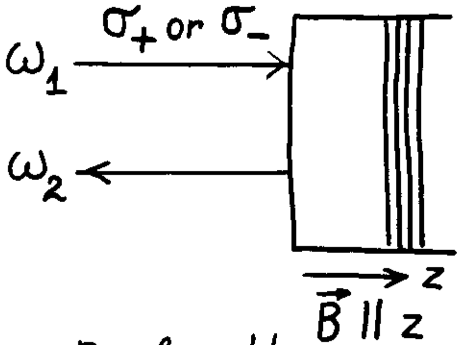

Backscattering Faraday geometry

$$\hbar|\omega_2 - \omega_1| = g_A \mu_0 B$$

(A) The long-wavelength edge

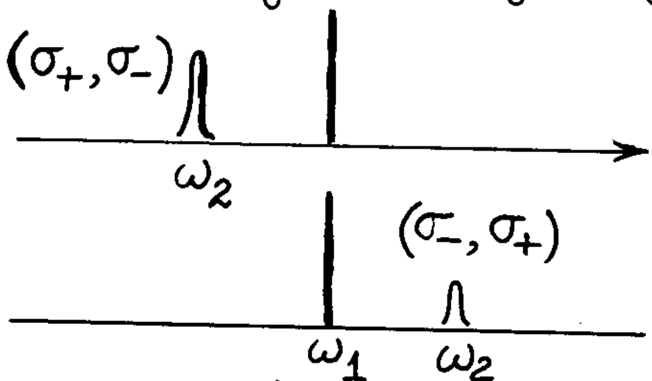

(B) The short-wavelength edge

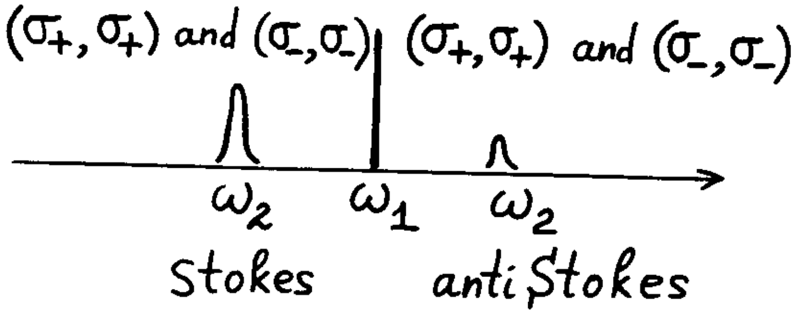

Two different scattering mechanisms

(A)

$$\left|\tfrac{3}{2}\right\rangle_A \overset{\sigma_-}{\left|\tfrac{1}{2}, -\tfrac{3}{2}\right\rangle} \longrightarrow \left|-\tfrac{3}{2}\right\rangle_A \overset{\sigma_+}{\left|-\tfrac{1}{2}, \tfrac{3}{2}\right\rangle}$$

$$\left|-\tfrac{3}{2}\right\rangle_A \underset{\sigma_+}{\left|-\tfrac{1}{2}, \tfrac{3}{2}\right\rangle} \longrightarrow \left|\tfrac{3}{2}\right\rangle_A \underset{\sigma_-}{\left|\tfrac{1}{2}, -\tfrac{3}{2}\right\rangle}$$

(B)

$$\left|\tfrac{3}{2}\right\rangle_A \left|\tfrac{1}{2}, -\tfrac{3}{2}\right\rangle \longrightarrow \left|-\tfrac{3}{2}\right\rangle_A \left|\tfrac{1}{2}, -\tfrac{3}{2}\right\rangle$$

$$\left|-\tfrac{3}{2}\right\rangle_A \underset{\sigma_-}{\left|\tfrac{1}{2}, -\tfrac{3}{2}\right\rangle} \longrightarrow \left|\tfrac{3}{2}\right\rangle_A \underset{\sigma_-}{\left|\tfrac{1}{2}, -\tfrac{3}{2}\right\rangle}$$

SPIN-FLIP RAMAN SCATTERING-2

B-type scattering (the intermediate state is a neutral acceptor with a neighboring localized exciton)

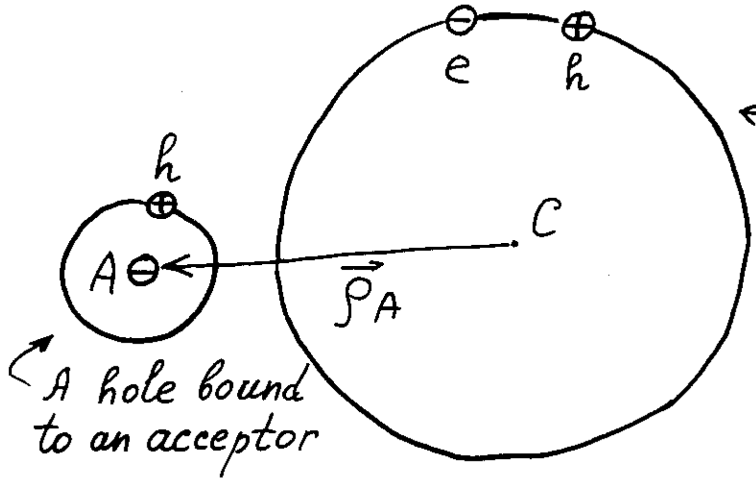

The mechanism B is contributed by flip-stop exchange interaction

$$\underset{h,A}{\pm 3/2} + \underset{h,exc}{m} \longrightarrow \underset{h,A}{\mp 3/2} + \underset{h,exc}{m}$$

or $\quad \sigma_z^{(h,exc)}\left(\Delta_+\sigma_+^{(h,A)} + \Delta_-\sigma_-^{(h,A)}\right) \quad$, where $\Delta_- = \Delta_+^*$,

$$\sigma_+ = \begin{array}{c c} & \begin{array}{cc} 3/2 & -3/2 \end{array} \\ \begin{array}{c} 3/2 \\ -3/2 \end{array} & \begin{bmatrix} 0 & 1 \\ 0 & 0 \end{bmatrix} \end{array}, \quad \sigma_- = \begin{bmatrix} 0 & 0 \\ 1 & 0 \end{bmatrix}, \quad \sigma_z = \begin{bmatrix} 1 & 0 \\ 0 & -1 \end{bmatrix}$$

Note that the usual flip-flop exchange interaction

$$\underset{h,A}{(\pm 3/2)} + \underset{h,exc}{(\mp 3/2)} \rightarrow \underset{h,A}{(\mp 3/2)} + \underset{h,exc}{(\pm 3/2)} \quad \text{or} \quad \left(\sigma_+^{(h,exc)}\sigma_-^{(h,A)} + \sigma_-^{(h,exc)}\sigma_+^{(h,A)}\right)$$

does not contribute to the scattering B

$$\Delta_\pm = \Delta(\rho)\,(\rho_x \mp i\rho_y)^3\,, \quad \Delta(\rho) \to 0 \ \text{ as } \rho \to \infty$$

TABLE I. Parameters of the GaAs/Al_xGa_{1-x}As MQW samples and the measured g factors of excitons and holes.

Well-barrier width (Å)	x	Doping $\times 10^{16}$ cm^{-3}	Periods	Exciton g factor	Hole g factor
46/110	0.33	7	100	1.1(1)	2.3(1)
72/110	0.33	5	100		2.1(1)
102/110	0.33	5	100		2.0(1)
29/101	0.34		150	1.5(1)	
71/104	0.33		70	1.0(1)	
98/103	0.35		40	0.8(1)	
198/103	0.35		25		

A-type scattering (the intermediate state is an exciton bound to a neutral acceptor, or A^0X)

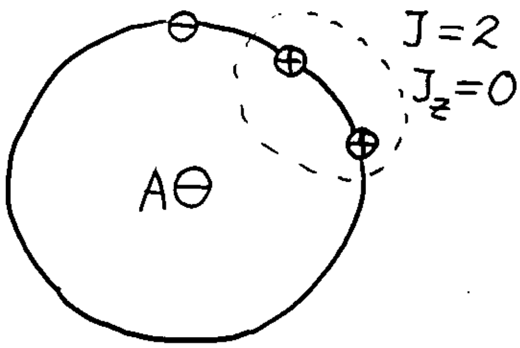

$$(A,-\tfrac{3}{2}) + \sigma_+ \xrightarrow{\text{Light absorption}} \underset{h\ \ h}{\overset{e,\,-1/2}{(+3/2,-3/2)}} \Longrightarrow \underset{h\ \ h}{\overset{e,\,1/2}{(+3/2,-3/2)}} + \text{acoustic phonon}$$

$$\xrightarrow[\text{Light emission}]{} (A,\tfrac{3}{2}) + \text{acoustic phonon} + \sigma_-$$

$$\hbar\omega_1 - \hbar\omega_2 = g_A \mu_0 B \cos\theta + \underbrace{(-g_e)\mu_0 B}_{\text{Energy of the acoustic phonon}}$$

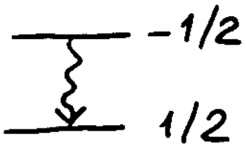

$$\hbar\Omega_{ac.phon.} = (-g_e)\mu_0 B$$

At oblique magnetic fields, the selection rules are weakened and the A-scattering can also take place without participation of an acoustic phonon. In this case,

$$\hbar\omega_1 - \hbar\omega_2 = g_A \mu_0 B \cos\theta$$

θ is the angle between z and $\vec{B}$

Spin-flip Raman scattering-4

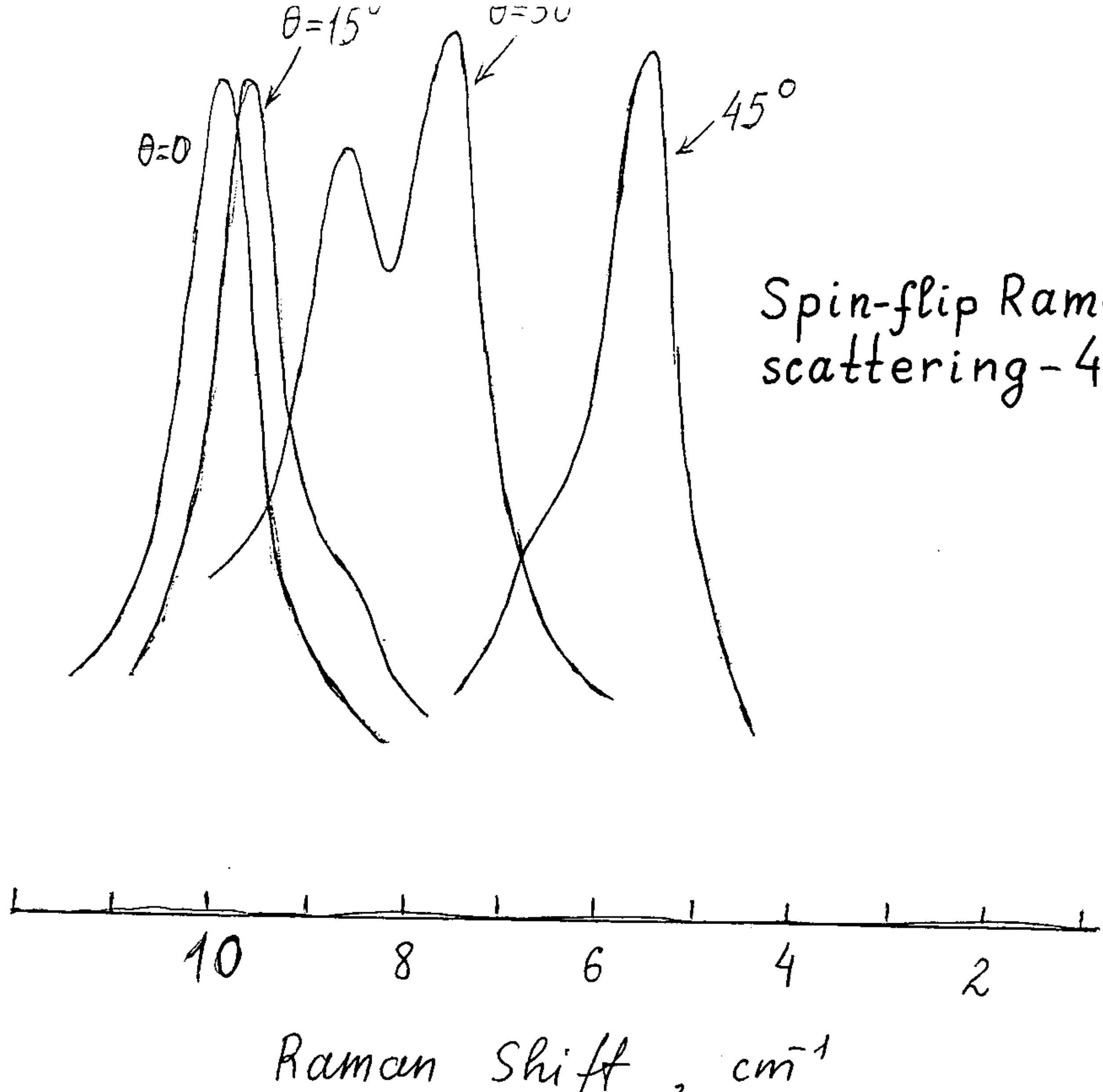

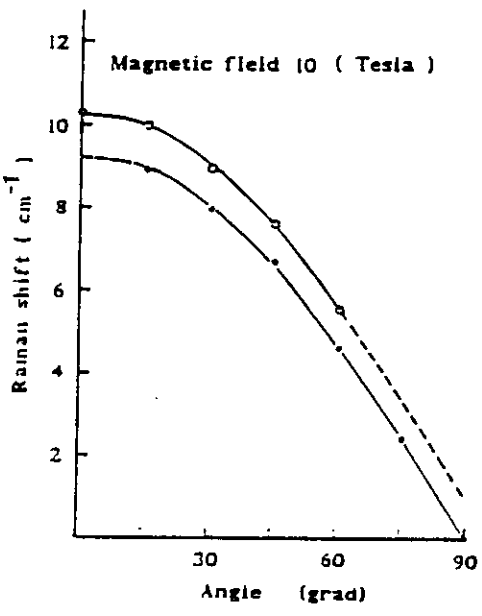

Fig.2 Dependence of the $-3/2 \longrightarrow 3/2$ SFRS line on the angle between field and growth direction.